THE JOURNAL OF BIOLOGICAL CHEMISTRY VOL. 283, NO. 30, pp. 20925–20936, July 25, 2008

Studies with the Human Cohesin Establishment Factor, ChlR1

*ASSOCIATION OF ChlR1 WITH Ctf18-RFC AND Fen1**

Received for publication, April 8, 2008, and in revised form, May 21, 2008 Published, JBC Papers in Press, May 21, 2008, DOI 10.1074/jbc.M802696200

Andrea Farina[‡], Jae-Ho Shin[§], Do-Hyung Kim[¶], Vladimir P. Bermudez[‡], Zvi Kelman[§], Yeon-Soo Seo[¶1], and Jerard Hurwitz[‡2]

From the [‡]Program of Molecular Biology, Memorial Sloan Kettering Cancer Center, New York, New York 10065, the [§]University of Maryland Biotechnology Institute, Rockville, Maryland 20850, and the [¶]Department of Biological Sciences, Korea Advanced Institute of Science and Technology, Daejeon, 305-701, Korea

Human ChlR1 (hChlR1), a member of the DEAD/DEAH subfamily of helicases, was shown to interact with components of the cohesin complex and play a role in sister chromatid cohesion. In order to study the biochemical and biological properties of hChlR1, we purified the protein from 293 cells and demonstrated that hChlR1 possesses DNA-dependent ATPase and helicase activities. This helicase translocates on single-stranded DNA in the 5′ to 3′ direction in the presence of ATP and, to a lesser extent, dATP. Its unwinding activity requires a 5′-single-stranded region for helicase loading, since flush-ended duplex structures do not support unwinding. The helicase activity of hChlR1 is capable of displacing duplex regions up to 100 bp, which can be extended to 500 bp by RPA or the cohesion establishment factor, the Ctf18-RFC (replication factor C) complex. We show that hChlR1 interacts with the hCtf18-RFC complex, human proliferating cell nuclear antigen, and hFen1. The interactions between Fen1 and hChlR1 stimulate the flap endonuclease activity of Fen1. Selective depletion of either hChlR1 or Fen1 by targeted small interfering RNA treatment results in the precocious separation of sister chromatids. These findings are consistent with a role of hChlR1 in the establishment of sister chromatid cohesion and suggest that its action may contribute to lagging strand processing events important in cohesion.

In order to maintain genomic integrity, the two sister chromosomes synthesized in S phase must be linked together physically by the cohesin complex until they are distributed to daughter cells in anaphase. Cohesion is mediated by cohesin, a ring-shaped protein complex composed of the four subunits, Smc1, Smc3, Scc3, and the kleisin Scc1/Mdc1/Rad21 (1–4). In budding yeast, cohesion establishment factors, which include minimally Chl1, Ctf7/Eco1/Eso1, Ctf4/Pob1/AND-1, Ctf18/Chl12, Dcc1, and Ctf8, are essential for cohesion, and all play some role in DNA replication (5–12). The *CHL1* (chromosome loss mutation) gene was first isolated in a screen in *Saccharomyces cerevisiae* for mutants exhibiting unusual mating phenotypes due to the loss of chromosome III (13, 14). *Chl1* null mutants, although viable, show a G_2/M cell cycle delay and ~200-fold increase in the rate of chromosome III missegregation due to both sister chromatid loss and sister chromatid nondisjunction, confirming that the protein it encodes, Chl1p, is required for the maintenance of correct chromosome transmission (15). A functional ATP-binding motif in Chl1p is essential for normal chromosome segregation, since overexpression of Chl1p mutants defective in ATP binding interfere with high fidelity chromosome transmission (16). Humans have two *CHL1*-related genes, *DDX11* and *DDX12*, which encode the proteins ChlR1 and ChlR2, respectively. Although the function of ChlR2 is unclear, human ChlR1 (hChlR1),[3] a protein with a predicted molecular mass of 102 kDa, has 33% identity and 50% homology to Chl1p of budding yeast (17).

Although the exact role of Chl1p in cohesion establishment remains unclear, recent studies in yeast and higher eukaryotes have substantiated that Chl1p is involved in this process. In budding yeast, Chl1p associates physically with Ctf7p (18) and genetically with Ctf18, two proteins essential for the establishment of cohesion. Ctf7p is necessary for the establishment of cohesion during DNA replication but is not involved directly in holding sister chromatids together (8, 10). Unlike Ctf7, Ctf18 is not essential in budding yeast, but in its absence, sister chromatid cohesion is compromised (6, 7). Ctf18, Dcc1, and Ctf8 form a complex with the four small subunits of replication factor C (RFC) in yeast and humans. RFC is a five-subunit complex that catalyzes the loading of PCNA onto DNA, which confers processivity to both DNA polymerases δ and ϵ during DNA replication (reviewed in Ref. 19). In the Ctf18-RFC complex, the RFC1 subunit is replaced by Ctf18, Dcc1, and Ctf8. As observed with RFC, Ctf18-RFC also loads PCNA onto DNA (20–22). Ctf18, together with Ctf7 and Ctf4, localize to the replication fork (23), adding further evidence that cohesion is linked to DNA replication. Interestingly, deletion of either *CTF8* or *CHL1* results in abnormal sister chromatid cohesion (24, 25), whereas deletion of both genes (as well as the simultaneous

* This work was supported, in whole or in part, by National Institutes of Health Grants GM 34559 and GM 27440 (to J. H.). This work was also supported by American Cancer Society Research Scholar Grant RSG-04-050-01-GMC (to Z. K.). The costs of publication of this article were defrayed in part by the payment of page charges. This article must therefore be hereby marked "*advertisement*" in accordance with 18 U.S.C. Section 1734 solely to indicate this fact.

[1] Present address: School of Applied Biosciences, Kyungpook National University, Daegu 702-701, Republic of Korea.

[2] To whom correspondence should be addressed: 1275 York Ave., Box 97, New York, NY 10065. Tel.: 212-639-5896; Fax: 212-717-3627; E-mail: j-hurwitz@ski.mskcc.org.

[3] The abbreviations used are: hChlR1, human ChlR1; RFC, replication factor C; siRNA, small interfering RNA; HA, hemagglutinin; PCNA, proliferating cell nuclear antigen; FISH, fluorescence *in situ* hybridization; DTT, dithiothreitol; PMSF, phenylmethylsulfonyl fluoride; nt, nucleotide(s); AMP-PNP, 5′-adenylyl-β,γ-imidodiphosphate; ATPγS, adenosine 5′-*O*-(thiotriphosphate); ssDNA, single-stranded DNA.

deletion of different pairs of establishment factors) is lethal (18, 24). In human cells, siRNA experiments revealed that hChlR1 interacts with cohesin components and is required for sister chromatid cohesion (26). Recently, it was reported that in *Ddx11*$^{-/-}$ mouse embryos, ChlR1 is necessary for the cohesion of both chromosome arms and centromeres (27).

In this report, we have purified hChlR1 and characterized its biochemical properties as an ATP-dependent DNA helicase. We also show that hChlR1 interacts with human Ctf18-RFC and Fen1. Biochemical analyses revealed that the length of the duplex region displaced by the helicase activity of hChlR1 was increased by Ctf18-RFC and that the flap endonuclease activity of Fen1 was increased by hChlR1. Furthermore, we show that siRNA depletion of hChlR1 in HeLa cells, as well as Fen1, leads to increased sister chromatid separation, similar to that observed following depletion of the cohesin subunit Scc1. We posit that the action of some of the establishment factors may involve the processing of lagging strands during cohesion.

EXPERIMENTAL PROCEDURES

DNA, Nucleotides, Enzymes, and Antibodies—M13mp18(+) single-stranded circular DNA was purchased from New England Biolabs. The oligonucleotides used were synthesized commercially by Integrated DNA Technologies (Coralville, IA). Unlabeled dNTPs and NTPs were obtained from Roche Applied Science and Promega, respectively. Labeled dNTPs and NTPs were purchased from PerkinElmer Life Sciences. Human RPA, PCNA, Ctf18-RFC, and RFC complexes were isolated as described (20, 28). Mouse monoclonal M2 anti-FLAG and anti-HA antibodies were from Sigma. The rabbit polyclonal antiserum to the hChlR1 protein (Hel1) was obtained from J. M. Lahti (17), whereas rabbit antisera against hCtf18, Dcc1, and 37-kDa RFC subunits have been described (20, 29). The RFC p140 monoclonal antibody was kindly supplied by B. Stillman. Mouse monoclonal against PCNA (PC-10) and α-tubulin were purchased from Santa Cruz Biotechnology, Inc. (Santa Cruz, CA) and Calbiochem, respectively; rabbit polyclonal Scc1 (Rad21 BL331) and Fen1 antibodies were purchased from Bethyl Laboratories and Novus Biologicals, respectively.

Plasmids—Human ChlR1 cDNA in pcDNA3 (Invitrogen), obtained from Dr. J. M. Lahti (Department of Genetics and Tumor Cell Biology, St. Jude Children's Research Hospital, Memphis, TN), was subjected to PCR using primers ChlR1-NotI (5′-ATAAGAATGCGGCCGCCATGGCTAATGAAACACAGAAGG-3′) and ChlR1-NotI-M (5′-ATAGTTTAGCGGCCGCTCAGGAAGAGGCCGACTTCTC-3′), which amplified the gene devoid of the extra HA sequence, or with primers ChlR1-NotI and ChlR1-NotI-L (5′-ATAGTTTAGCGGCCGCTCAGGAAGAGGCCGACTTCTCCCGGTGAAACTTCTGCAC-3′), which amplified the gene and included the HA sequence. Both PCR products were subcloned into the NotI site of pIRESpuro2-His$_6$-FLAG$_2$ (Clontech). The sequences of the resulting plasmids, pIRESpuro2::His$_6$-FLAG$_2$-ChlR1 and pIRESpuro2::His$_6$-FLAG$_2$-ChlR1-HA, were verified. pIRESpuro2::His$_6$-FLAG$_2$-FEN1 was prepared as follows. The human FEN1 cDNA in pET-23d vector (Novagen) was amplified by PCR using primers 5′FEN1-NotI (5′-ATAAGAATGCGGCCGCGGGAATTCAAGGCCTGGCCA-3′) and 3′FEN1-NotI (5′-ATAGTTTAGCGGCCGCTTATTTTCCCCTTTTAAACTTCC-3′). PCR products were subcloned into the NotI site of pIRESpuro2-His$_6$-FLAG$_2$ (Clontech). The resulting plasmid, pIRESpuro2::His$_6$-FLAG$_2$-FEN1, was sequenced to verify that no mutations were introduced during PCR and cloning. hCtf18, Dcc1, and Ctf8 were subcloned into pIRESpuro2-His$_6$-FLAG$_2$ (Clontech), as described (20). The plasmid containing the centromeric region of chromosome 9 was used as the probe in the FISH analyses (a gift from Dr. M. A. Lavershа, Molecular Cytogenetics Core Facility, Memorial Sloan Kettering Cancer Center, New York, NY) and was previously described (30).

hChlR1 Expression and Purification—hChlR1 cDNA in pIRESpuro2::His$_6$-FLAG$_2$ plasmids was transfected into 293 cells using Lipofectamine 2000 (Invitrogen), as recommended by the manufacturer, and cells were grown and selected in Dulbecco's modified Eagle's medium containing 10% (v/v) fetal bovine serum and 2.5 μg/ml of puromycin for 2 weeks. Selected cells were analyzed for the expression of His-FLAG-ChlR1 by Western blot analyses. A single clone of 293 cells expressing His-FLAG-ChlR1 was grown in 4 liters of Joklik medium with 10% (v/v) fetal bovine serum and 2.5 μg/ml puromycin. Cells were harvested by centrifugation at 600 × *g* at 4 °C for 10 min. Packed cells (10 ml) were washed with ice-cold PBS and resuspended in 20 ml of hypotonic buffer (10 mM Tris·HCl, pH 7.4, 10 mM KCl, 1.5 mM $MgCl_2$, 1 mM DTT, 0.5 mM phenylmethylsulfonylfluoride (PMSF), proteinase inhibitors (2 μg/ml aprotinin, 2 μg/ml leupeptin, 2 μg/ml antipain, and 0.1 mM benzamidine)) on ice for 15 min. Cells were lysed by Dounce homogenization (7 strokes), and the mixture was centrifuged at 4 °C for 30 min at 2,400 × *g*. The nuclear pellet was resuspended in 10 ml of 0.15 M NaCl buffer (20 mM Tris·HCl, pH 7.4, 0.15 M NaCl, 10% glycerol, 1.5 mM $MgCl_2$, 0.2 mM EDTA, 1 mM DTT, 0.5 mM PMSF, proteinase inhibitors) and incubated with rocking at 4 °C for 30 min. The nuclear fraction was centrifuged at 4 °C for 30 min at 43,500 × *g*. Half of the supernatant (8 ml, 25 mg of protein) was incubated with 1 ml of FLAG-M2-agarose resin (Sigma) in FLAG buffer (20 mM Tris·HCl, pH 7.4, 0.15 M NaCl, 10% glycerol, 0.05% Nonidet P-40, 1.5 mM $MgCl_2$, 0.2 mM EDTA, 0.5 mM PMSF, proteinase inhibitors) at 4 °C overnight. The resin was packed onto a column and washed three times with 10 ml of FLAG buffer, and bound proteins were eluted five times with 0.4 ml of FLAG buffer containing 1 mg/ml of $FLAG_3$ peptide for 1 h at 4 °C (yielding 0.5 mg of protein). An aliquot of the pooled FLAG peptide-eluted fraction (0.2 ml; 50 μg of protein) was layered onto a 5-ml 15–40% glycerol gradient containing 25 mM Tris·HCl (pH 7.5), 1 mM EDTA, 0.15 M NaCl, 1 mM DTT, 0.01% Nonidet P-40, and proteinase inhibitors and centrifuged at 250,000 × *g* for 20 h at 4 °C, and fractions (0.15 ml each) collected from the bottom of the tube (yielding 10 μg of relatively pure protein). The His-FLAG-ChlR1 protein was detected by Coomassie staining and sedimented between aldolase (7.8 S) and bovine serum albumin (4.41 S).

Preparation of Helicase Substrates—Oligonucleotides used for the preparation of the different helicase substrates are summarized in Table 1. The indicated oligonucleotides, 18mer-M13 and 39mer-M13, are complementary to nucleotides

TABLE 1
Oligonucleotides used in this study

Oligonucleotide	Sequence (length of oligonucleotide)
18mer-M13	5′-TTTTTTTTTTTTTTTTTTTTCAGGGTTTTCCCAGTCAC-3′ (38 nt)
39mer-M13	5′-TTTTTTTTTTTTTTTTTTTTGATTAAGTTGGGTAACGCCAGGGTTTTCCCAGTCACGAC-3′ (59 nt)
39mer40dTM13	5′-TTTTTTTTTTTTTTTTTTTTTTTTTTTTTTTTTTTTTTTTTGATTAAGTTGGGTAACGCCAGGGTTTTCCCAGTCACGAC-3′ (79 nt)
D50	5′-GGGACGCGTCGGCCTGGCACGTCGGCCGCTGCGGCCAGGCACCCGATGGC-3′ (50 nt)
D75E	5′-GGGACGCGTCGGCCTGGCACGTCGGCCGCTGCGGCCTAGCATATGCTAGCCCGCTGCGGCCAGGCACCCGATGGC-3′ (75 nt)
D74	5′-GGGACGCGTCGGCCTGGCACGTCGGCCGCTGCGGCCAGGCACCCGATGGCGTTTGTTTGTTTGTTTGTTTGTTT-3′ (74 nt)
D50-5′	5′-CCGCTGCGGCCAGGCACCCGATGGCGGGACGCGTCGGCCTGGCACGTCGG-3′ (50 nt)
D55	5′-CCGACGTGCCAGGCCGACGCGTCCCTTTCTTTCTTTCTTTCTTTCTTTCTTTCTT-3′ (55 nt)
D25	5′-GCCATCGGGTGCCTGGCCGCAGCGG-3′ (25 nt)
D25F	5′-CCGACGTGCCAGGCCGACGCGTCCC-3′ (25 nt)
G49	5′-GCCATCGGGTGCCTGGCCGCAGCGGTTTGTTTGTTTGTTTGTTTGTTTG-3′ (49 nt)
G45	5′-CATATGCTAGGCCGCAGCGGCCGACGTGCCAGGCCGACGCGTCCC-3′ (45 nt)
G40	5′-GCTAGGCCGCAGCGGCCGACGTGCCAGGCCGACGCGTCCC-3′ (40 nt)
729	5′-CGAACAATTCAGCGGCTTTAACCGGACGCTCGACGCCATTAATAATGTTTTC-3′ (52 nt)
5TY-1	5′-GAAAACATTATTAATGGCGTCGAGCTAGGCACAAGGCGAACTGCTAACGG-3′ (50 nt)
5TBG	5′-CCGTTAGCAGTTCGCCTTGTGCCTAG-3′ (26 nt)

6313–6330 and 6310–6348 of M13mp18(+) DNA, respectively. The helicase substrates were labeled (as indicated in the figures by an *asterisk*) at either the 3′- or the 5′-ends. For the preparation of substrates, 3′-end-labeled oligonucleotides (1 pmol) were annealed with 2.5 μg (1 pmol) of ssM13mp18 DNA in a buffer containing 50 mM NaCl and 1 mM EDTA by heating to 100 °C for 3 min followed by slow cooling to 25 °C. The 3′-end of the annealed oligonucleotides was labeled by an extension reaction using Klenow and [α-^{32}P]dGTP (6,000 Ci/mmol). Excess labeled nucleotides and unannealed oligonucleotides were removed by Sepharose CL-4B column chromatography. 5′-End-labeled substrates were prepared with T4 polynucleotide kinase and [γ-^{32}P]ATP (3000 Ci/mmol), and reactions were halted with EDTA (final concentration, 25 mM). Labeled oligonucleotides were hybridized to complementary oligonucleotides (at a 1:1 molar ratio) in 40 mM Hepes-NaOH (pH 7.5) and 50 mM NaCl by heating to 100 °C for 3 min, followed by slow cooling to 25 °C. Unincorporated [γ-^{32}P]ATP and unannealed oligonucleotides were removed by electrophoresis through an 8% native polyacrylamide gel as described (31).

To determine the maximal length of duplex DNA displaced by the hChlR1 helicase, substrates containing longer duplex regions were prepared by elongating singly primed M13mp18 ssDNA (39mer40dT-M13) using Sequenase (U.S. Biochemical Corp.), as described (32).

DNA Helicase Assay—Helicase activity was measured in reactions (15 μl) containing 25 mM Hepes-NaOH (pH 7.5), 25 mM potassium acetate, 1 mM magnesium acetate, 1 mM ATP, 1 mM DTT, 100 μg/ml bovine serum albumin, 5 fmol of ^{32}P-labeled substrate (3,000 cpm/fmol), and enzyme fractions, as indicated in figure legends. After incubation at 37 °C for 30 min, reactions were stopped with 3 μl of 6× stop solution (50 mM EDTA, 2% SDS, 40% glycerol, 0.3% bromphenol blue, and 0.3% xylene cyanol), and aliquots were loaded on a 12% polyacrylamide gel in 1× TBE and electrophoresed for 90 min at 55 V. Reaction mixtures from assays used to measure processivity were electrophoresed through a 2.5% agarose gel in 1× TBE at 120 V for 3 h. Displaced bands were visualized and quantitated by phosphorimaging.

ATPase Assay—Reaction mixtures (20 μl) containing 25 mM Tris-HCl (pH 7.5), 3 mM magnesium acetate, 2 mM DTT, 200 μg/ml bovine serum albumin, 50 μM ATP, 30 nM [γ-^{32}P]ATP (3000 Ci/mmol), 40 fmol of M13mp18 ssDNA, or other polynucleotides and varying levels of hChlR1 were incubated at 37 °C, as indicated. Aliquots (0.5 μl) were spotted onto polyethyleneimine-cellulose TLC plates (Merck) that were then developed in 0.5 M LiCl, 1.0 M formic acid. Products formed were analyzed using a PhosphorImager.

Immunoprecipitations—293 cells or 293 cells constitutively expressing His-FLAG-ChlR1-HA were grown in a 100-mm dish and transfected with the indicated constructs using Lipofectamine 2000 (Invitrogen). Cells were washed once in PBS and incubated in 0.2 ml of hypotonic buffer (10 mM Tris·HCl (pH 7.5), 10 mM KCl, 1.5 mM $MgCl_2$, 1 mM DTT, 0.5 mM PMSF, and proteinase inhibitors) for 15 min on ice. Nonidet P-40 was added (final concentration, 0.6%), and the lysate was centrifuged at 1,500 × *g* for 30 s at 4 °C. Nuclear pellets were resuspended in buffer C (20 mM Tris·HCl (pH 7.4), 150 mM NaCl, 0.05% Nonidet P-40, 10% glycerol, 1.5 mM $MgCl_2$, 0.2 mM EDTA, 1 mM DTT, 0.5 mM PMSF, and proteinase inhibitors) with rocking for 30 min at 4 °C. After centrifugation at 38,000 × *g*, nuclear extracts were treated with 20 μg/ml DNase I and then incubated with anti-FLAG (M2) or anti-HA beads (20 μl) at 4 °C for 4 h. Alternatively, Ctf18 and Fen1 were immunoprecipitated with 1 μl of their respective antisera from lysates using the same conditions described above, and 20 μl of Protein A-agarose (Upstate Biotechnology) was added. After centrifugation, beads were washed three times with buffer C, and bound proteins were eluted with SDS loading buffer followed by SDS-PAGE separation on 4–20% gels (Ctf18, Ctf8, Dcc1, PCNA, and RFC1 co-immunoprecipitations) or 8% gels (Fen1 co-immunoprecipitations) and immunoblot analysis.

siRNA Experiments—The 21-mer siRNAs with 3′ dT overhangs that targeted hChlR1, FEN1, SCC1, and a negative control, were synthesized by Qiagen and delivered into cells at a final concentration of 100 nM using Lipofectamine 2000 (Invitrogen). The nucleotides targeted by the siRNA were as follows: in hChlR1, 212–232; in FEN1, 1766–1786; in SCC1, 142–162. As a negative control, the random sequence targeted by the siRNA was 5′-AATTCTCCGAACGTGTCACGT-3′.

Chromosome Spreads, FISH Analysis, and Microscopy—HeLa cells were transfected with siRNA oligonucleotides specific for hChlR1, Fen1, or Scc1 or with the negative control

siRNA and incubated for 48 h. Cells were then blocked with 0.5 μg/ml nocodazole for 2 h and swelled in hypotonic buffer (75 mM KCl) for 15 min at 37 °C. Cells were fixed in 75% methanol, 25% acetic acid, and spreads were prepared by dropping suspended cells onto slides, which were then stained with 0.2 μg/ml 4′,6-diamidino-2-phenylindole or used for FISH analysis, as described (33). Images collected with an Olympus AX70 microscope were processed using MetaMorph software.

RESULTS

Helicase and ATPase Activities of hChlR1—In order to study the biochemical properties and activities associated with hChlR1, we purified and characterized the recombinant protein. Initial efforts to express hChlR1 in bacteria or insect cells failed due to poor expression, extensive degradation, and/or aggregation. In contrast, expression of the protein in human cells yielded full-length and soluble hChlR1. To facilitate its production and isolation, stable 293 cell lines were generated that expressed His-FLAG-ChlR1 (or His-FLAG-ChlR1-HA, used in some co-immunoprecipitation experiments). His-FLAG-ChlR1 was purified by FLAG immunoprecipitation, followed by glycerol gradient sedimentation, as described under "Experimental Procedures." We verified that the purified tagged protein was hChlR1 by Western blot analysis using either anti-ChlR1 (Fig. 1*A*) or anti-FLAG antibodies (data not shown). The protein detected had a molecular mass of ~120 kDa, a size expected for the His-FLAG-hChlR1 fusion protein. Site-directed mutagenesis, which changed the lysine residue at amino acid 50 to arginine (the Walker A box of the ATP binding motif), generated an enzymatically inactive hChlR1 (KR mutant) protein, which was previously described (34). The KR mutant of hChlR1 (hChlR1-KRm) was cloned into a mammalian expression vector, and a stable 293 cell line that expressed His-FLAG-ChlR1-KRm was established as described for the wild-type protein and purified as described under "Experimental Procedures" (Fig. 1*A*).

The helicase activity associated with purified hChlR1 was evaluated using a ^{32}P-labeled DNA substrate containing ssM13mp18 DNA hybridized to an 18-nt complementary labeled oligonucleotide with a 20-nt oligo(dT) tail at its 5′-end. This substrate was used to examine the activity of glycerol gradient fractions obtained in the purification of hChlR1 (Fig. 1*B*, *top*). Displacement of the ^{32}P-labeled oligonucleotide showed that the helicase activity and hChlR1 protein both eluted coincidentally (Fig. 1*B*, *middle*, fractions 17–19). We also examined the glycerol gradient fractions for DNA-dependent ATPase activity. As shown (Fig. 1*B*, *bottom*), this activity peaked with both the protein and helicase activity of hChlR1. In contrast, the hChlR1-KRm protein lacked both helicase and ATPase activity (34) (data not shown).

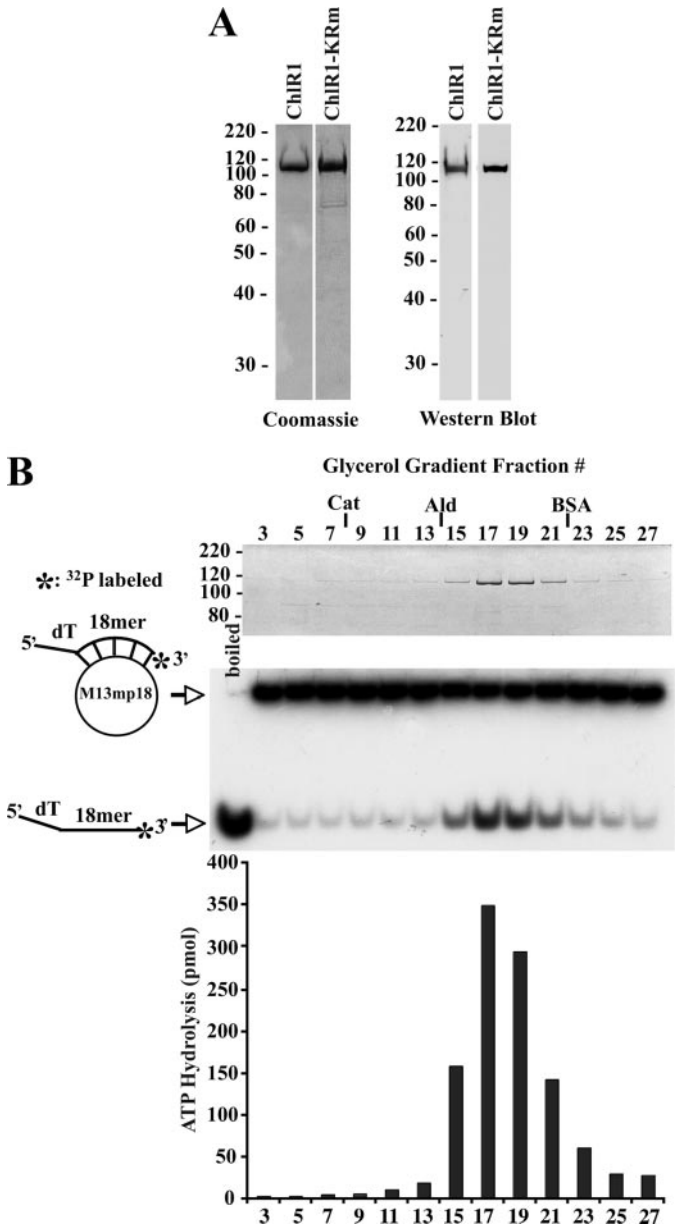

FIGURE 1. **Purification of recombinant hChlR1; examination of its helicase and ATPase activities.** Wild-type and mutant hChlR1 were overexpressed and purified from 293 cells as described under "Experimental Procedures." *A*, *left*, Coomassie-stained SDS-polyacrylamide gel of purified proteins (4 and 2 μg of hChlR1 and KRm, respectively); *right*, Western blot analysis of SDS-polyacrylamide gel using affinity-purified Hel1 antisera that recognizes the N terminus of the hChlR1 protein (200 ng of hChlR1 and KRm). *B*, cosedimentation of hChlR1 protein, DNA helicase, and DNA-dependent ATPase activities. *Top*, 50 μg of wild type hChlR1 protein was loaded onto a 5-ml 15–40% glycerol gradient; after centrifugation for 20 h at 250,000 × *g*, aliquots (2 μl) of the eluted fractions were assayed for helicase activity (*middle*) using the 18mer-M13 helicase substrate; DNA-dependent ATPase activity (*bottom*). *BSA*, bovine serum albumin.

Properties of hChlR1 Helicase Activity—We tested which nucleoside triphosphate supported hChlR1 helicase activity. As shown in Fig. 2*A*, this activity was observed with ATP and dATP but not with any other dNTPs (or NTPs; data not shown) tested. dATP supported the displacement of the 18-mer but not DNA substrates containing a duplex region of 39 nt. Furthermore, at low concentrations of hChlR1 (1–9 fmol), ATP was more effective than dATP in supporting the displacement of the 18-mer (Fig. 2*B*). DNA helicase activity of hChlR1 was not detected when ATP was replaced by nonhydrolyzable AMP-PNP or ATPγS (data not shown).

We next examined some of the biochemical properties of the hChlR1 helicase. We noted that maximal activity with Mg^{2+} was observed at low concentrations (0.5–1 mM), whereas higher levels (5 mM and above) markedly inhibited hChlR1 helicase activity more than 75% (data not presented). We also tested the

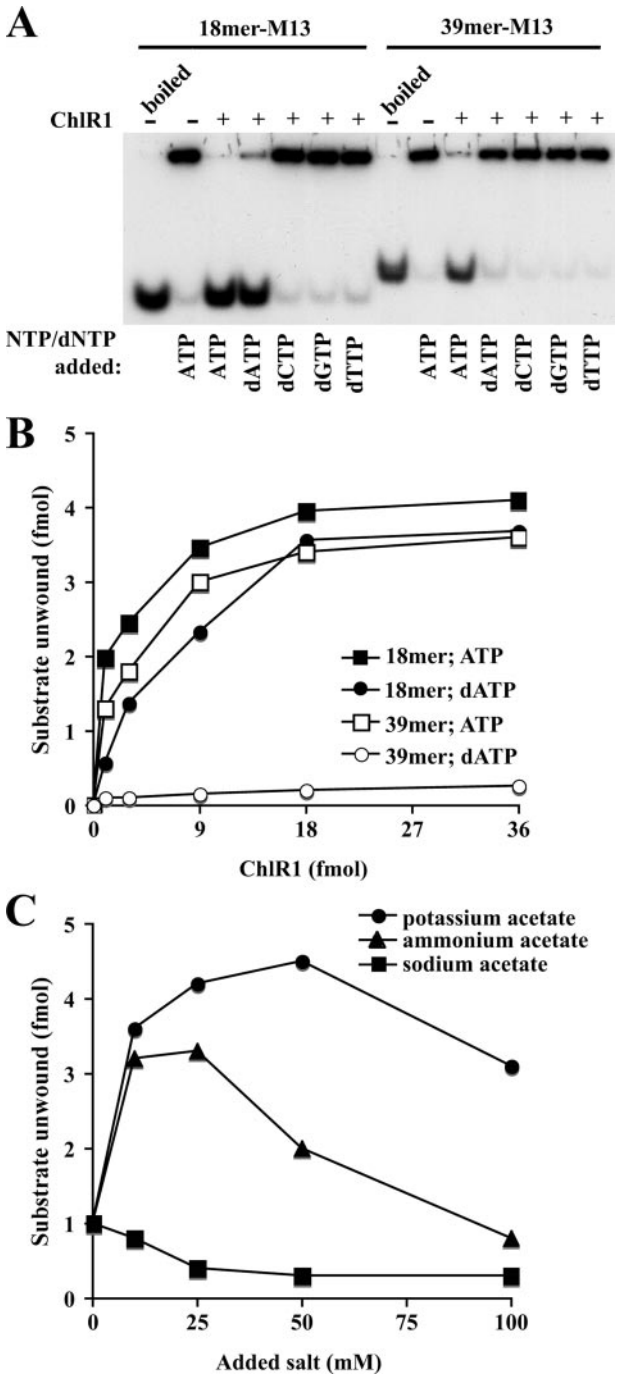

FIGURE 2. **Properties of hChlR1 helicase activity.** Helicase assays were carried out using conditions described under "Experimental Procedures." All reactions contained 36 fmol of hChlR1 and 5 fmol of the 39mer-M13 substrate, unless specified. *A*, nucleotide requirement for hChlR1 helicase activity. Each reaction contained, where noted, a 1 mM concentration of the indicated nucleoside 5′-triphosphate. *B*, unwinding of the 18mer-M13 or 39mer-M13 helicase substrate (18- and 39-mer, respectively) in the presence of increasing levels of hChlR1 and 1 mM ATP or dATP. *C*, the influence of various cations on hChlR1 helicase activity.

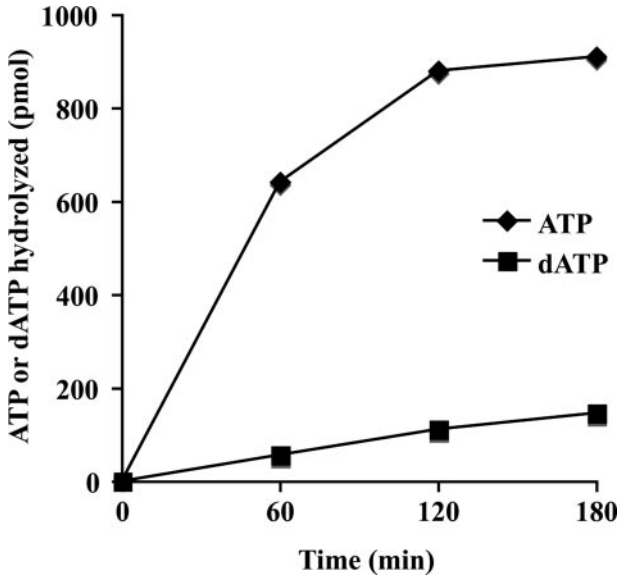

FIGURE 3. **Characterization of DNA-dependent ATPase activity of hChlR1.** Rate of hydrolysis of ATP and dATP by hChlR1. Reactions were carried out as described under "Experimental Procedures" in the presence of 90 fmol of hChlR1 and 40 fmol of the 18-mer M13 substrate.

effects of various salts and found that the helicase activity was stimulated by 25–50 mM potassium acetate, stimulated to a lesser extent by 25 mM of ammonium acetate, and markedly inhibited by sodium acetate (Fig. 2*C*). Since both Mg^{2+} and salt concentrations appeared critical, especially in the unwinding of long duplex regions, all subsequent experiments were carried out using the 39mer-M13 substrate or substrates with longer duplex regions in the presence of 1 mM Mg^{2+} and 25 mM potassium acetate. Under these conditions, the displacement activity of hChlR1 was maximal at pH 7.5 (data not shown). Using these optimal conditions, the helicase activity (using 36 fmol of protein) with the 39-nt duplex substrate proceeded linearly for 5 min and then plateaued at ~20 min (data not presented). Similar results were obtained with the 18-nt substrate (data not shown). In both cases, hChlR1 maximally displaced about 80% of the duplex substrates.

Properties of the hChlR1 ATPase Activity—All ATPase experiments were carried out in the absence or presence of either circular ssM13mp18 DNA or the partial duplex DNA substrates used in the helicase assays (39mer-M13; data not shown). ATPase activity was observed only in the presence of ssDNA and not with double-stranded DNA (data not shown). As expected, the Walker A mutated protein (KRm) contained no detectable ATPase activity (data not shown). ATP (and dATP) hydrolysis catalyzed by hChlR1 in the presence of a partial duplex DNA substrate was examined (Fig. 3). After 60 min of incubation, ATP was hydrolyzed ~12-fold more effectively than dATP. It should be noted that the DNA effector used in this experiment was the 18-nt M13 DNA substrate, which was unwound efficiently in the presence of either ATP or dATP (Fig. 2*A*). Possibly, the hChlR1-catalyzed unwinding of long duplex regions (39 nt and greater) in the presence of ATP but not dATP may be due to the marked differences in their hydrolysis, as shown in Fig. 3. We then tested whether different salt concentrations affected the ATPase activity of hChlR1. The addition of as little as 1 mM potassium acetate or ammonium acetate increased ATP hydrolysis about 2-fold (data not shown). In contrast to observations made in helicase assays, high salt levels (up to a 0.1 M concentration of the salts tested) stimulated the DNA-dependent ATPase activity of hChlR1 (data not presented), and potassium salts (glutamate, chloride,

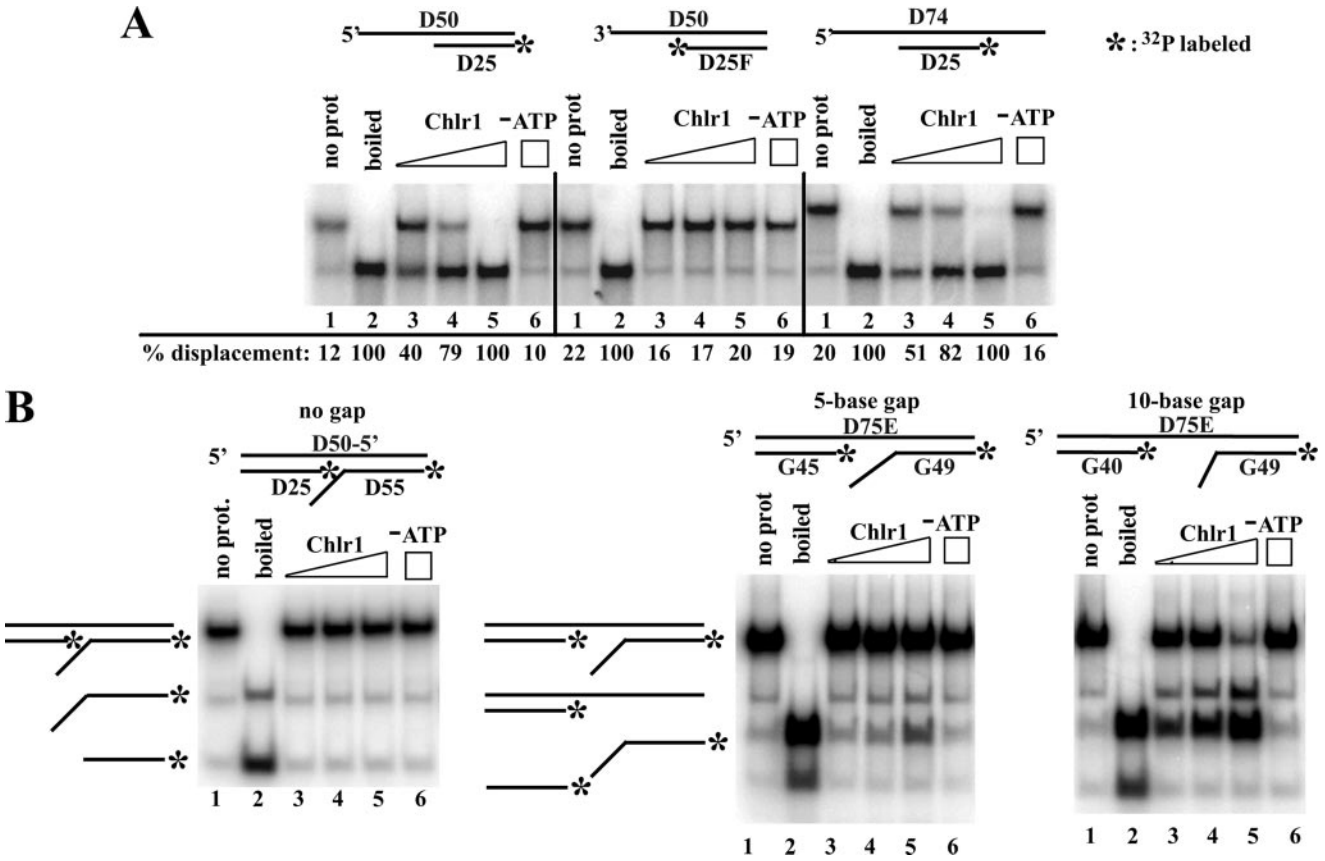

FIGURE 4. **Helicase activity of hChlR1 with various DNA substrates.** DNA helicase reactions were carried out as described under "Experimental Procedures" with increasing amounts of hChlR1 and 5 fmol of the indicated partial duplex DNA substrates. In all *panels* shown, the conditions used were as follows. *Lane 1*, substrate only; *lane 2*, boiled substrate; *lanes 3–5*, 1, 3, or 9 fmol of enzyme, respectively; *lane 6*, 9 fmol of enzyme but no ATP. *A*, hChlR1 helicase translocates in the 5′–3′ direction. *B*, displacement of nicked and gapped DNA substrates by hChlR1. The size of the single strand gap separating the two labeled oligonucleotide is noted *above* the *panels*. The sequences of oligonucleotides used to generate the substrates are noted, and their sequences are summarized in Table 1.

or acetate) were more effective than the corresponding sodium salts.

Directionality and Substrate Specificity—It was previously reported that hChlR1 translocated bidirectionally on ssDNAs, although a preference for the 5′–3′ direction was noted with substrates containing short ssDNA regions (34). We found that the enzyme translocated solely in the 5′–3′ direction on oligonucleotide substrates shown in Fig. 4*A*. The unwinding activity required a 5′-ssDNA region, since duplex structures containing a 5′ single-stranded tailed DNA hybridized to oligoribonucleotides were displaced, whereas 5′-single-stranded RNA hybridized to DNA oligonucleotides were not (data not shown). We also examined whether hChlR1 could unwind a duplex from a nick or a gapped region (Fig. 4*B*). Substrates containing a 10-nt gapped single-stranded region were unwound efficiently, similar to that observed with longer gapped single-stranded DNA regions (data not shown). However, substrates possessing a 5-nt gap or a nick were either displaced poorly or inactive even at high protein levels.

Length of Duplex Unwound by hChlR1 Is Stimulated by RPA—It was previously reported that hChlR1 purified from baculovirus-infected cells maximally displaced duplex regions of 20 bp (34). Under the experimental conditions described here, we noted that hChlR1 efficiently unwound longer duplex regions. In order to estimate the maximum duplex length displaced by the enzyme, a 5′-oligo(dT)-tailed M13 ssDNA helicase substrate (39mer40dT-M13) was prepared containing duplex regions that varied between 40 and 500 bp. Incubation of this DNA with increasing levels of hChlR1 resulted in the displacement of ssDNA that varied from 100 to ~400 nt in length (Fig. 5*A*, *lanes 4–6*). In the presence of RPA, both the level of helicase activity and extent of unwinding increased (Fig. 5*A*, *lanes 7–9*). This effect appeared specific for RPA, since *E. coli* SSB did not increase the displacement reaction (data not shown).

Length of Duplex Unwound by hChlR1 Is Stimulated by the Ctf18-RFC Complex—Cohesion requires the loading of cohesin onto DNA prior to the onset of replication. Once replication has commenced, establishment factors must act during S phase to achieve cohesion (6). In budding yeast, this group of proteins interacts genetically and physically with a number of replication proteins (18, 24, 25). Although their role in cohesion remains unclear, it is possible that the establishment factors act jointly to remodel newly replicated DNA near sites occupied by the cohesin complex. We tested whether some of the establishment factors influenced the helicase activity of hChlR1 by examining whether the unwinding reaction was affected by the addition of Ctf18-RFC complex (seven-subunit complex), Ctf7p, Dcc1p, Ctf8p, and Ctf4p, as well as RFC and PCNA. None of these factors alone or in combination increased the displacement observed with helicase substrates containing

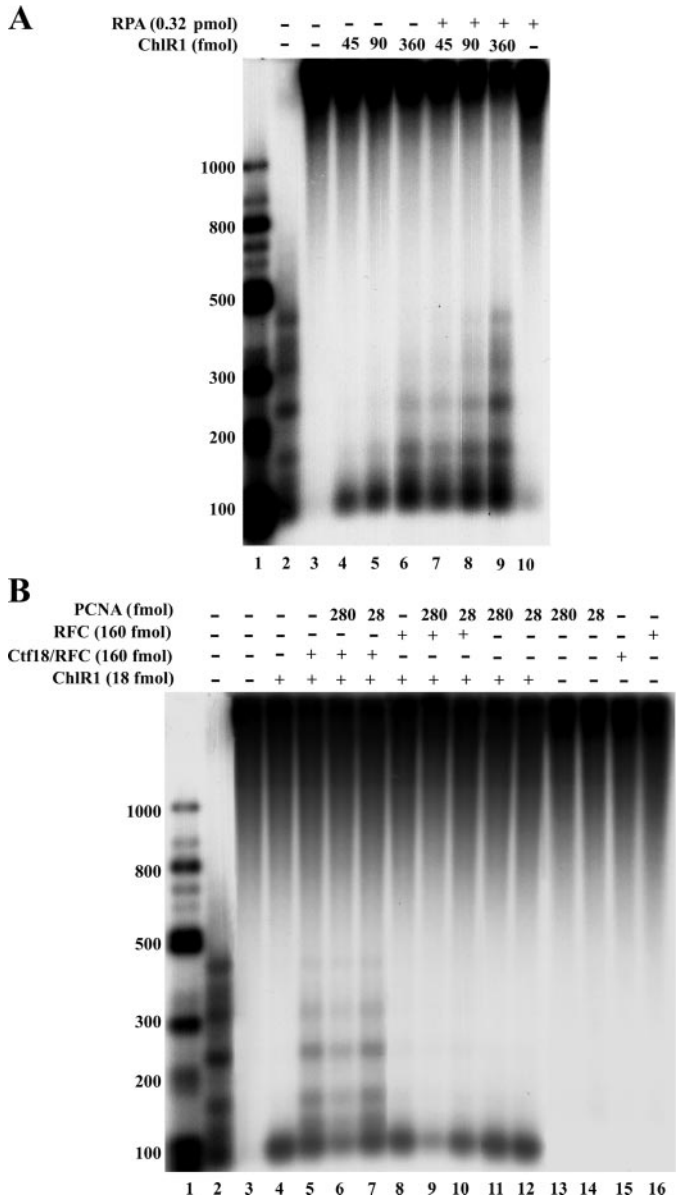

FIGURE 5. *A*, length of duplex unwound by hChlR1 is stimulated by RPA. DNA helicase activity was assayed using 5 fmol of the partial duplex M13 substrate (39mer40dT-M13, 5 fmol) containing duplex regions varying in length between 40 and 600 bp and a 40-nt oligo(dT) tail at its 5′-end. The indicated levels of hChlR1 were preincubated with the substrate in the standard helicase reaction but in the presence of 100 μM ATP, at 25 °C for 10 min, after which human RPA (0.32 pmol) was added as indicated, and all reactions were adjusted to 1 mM ATP. After incubation at 37 °C for 30 min, reactions were stopped by the addition of 20 mM EDTA, 0.1% SDS, 0.125 mg/ml proteinase K, and the mixture were incubated for an additional 30 min at 37 °C and then subjected to electrophoretic separation through a neutral 1% agarose gel. *Lane 1*, ^{32}P-labeled 100-bp ladder DNA marker (denatured); *lane 2*, boiled substrate; *lanes 3* and *10*, reactions without hChlR1; *lanes 4–6* and *7–9*, increasing amounts of hChlR1 in the absence or presence of RPA. *B*, length of duplex unwound by hChlR1 is stimulated by Ctf18-RFC. The hChlR1-catalyzed displacement reaction was carried out as described in *A*, with hChlR1 preincubation and the subsequent addition of Ctf18-RFC, RFC, or PCNA, as indicated.

duplex regions of 18, 25, and 39 bp (data not shown). We also tested whether these factors influenced the ability of hChlR1 to unwind long duplex regions. As shown in Fig. 5*B*, the addition of Ctf18-RFC increased the region displaced by hChlR1 from ~100 to ~500 bp (compare *lanes 4* and *5*). It should be noted that in this experiment, a low level of hChlR1 was added to minimize the displacement of regions longer than 100 nt. Both the seven- and five-subunit (devoid of Ctf8 and Dcc1) complexes of Ctf18-RFC were equally effective in supporting this reaction in a concentration-dependent manner, whereas RFC was much less effective than Ctf18-RFC in stimulating the displacement of longer chains (compare *lanes 5* and *8*). The molar ratio of Ctf18-RFC to hChlR1 used in the experiment described in the legend to Fig. 5*B* was ~9:1. Higher levels of Ctf18-RFC (1500 fmol) did not alter the unwinding reaction. However, significant stimulation of the displacement of DNA chains longer than 100 nt was observed at lower molar ratios, such as 1:1 and 2:1 (13 and 26%, respectively, of that shown in Fig. 5*B*). We suspect that the nonspecific binding of Ctf18-RFC to single-stranded M13 DNA may contribute to the relatively high concentration of Ctf18-RFC required to stimulate the extensive translocation activity of hChlR1. Although PCNA binds to hChlR1 (as discussed below), its addition did not affect the helicase-catalyzed displacement reaction (Fig. 5*B*, compare *lane 4* with *lanes 11* and *12*). Similarly, the addition of low levels of PCNA did not affect the activity observed in reactions containing Ctf18-RFC and hChlR1 (compare *lanes 5* and *7*), whereas higher PCNA levels were inhibitory (compare *lanes 5* and *6*). The addition of PCNA affected reactions with RFC similarly (*lanes 9* and *10*). None of the other establishment factors examined (Ctf4p, Ctf7p, Dcc1p, Ctf8p, and the Dcc1p-Ctf8p complex) affected the displacement reaction catalyzed by hChlR1 (data not shown).

In conclusion, these experiments show that Ctf18-RFC stimulated both the unwinding and extent of the displacement reaction catalyzed by hChlR1 helicase. Surprisingly, this effect was reduced by PCNA addition. The reasons for this effect remain to be explored further.

hChlR1 Interacts with Ctf18-RFC and PCNA—We tested whether these purified proteins interacted physically with hChlR1 as well as with RFC and PCNA. Weak interactions were detected between hChlR1 and either Ctf7 or Ctf4 (data not presented), whereas strong interactions were observed with Ctf18-RFC and PCNA. We investigated whether these interactions occurred *in vivo*. For this purpose, 293 cells were co-transfected with HA-tagged ChlR1 and, separately, with vectors expressing either the FLAG-tagged Ctf18 or Dcc1, subunit components of Ctf18-RFC. When lysates from these cells were treated with HA antibodies, hChlR1-HA co-immunoprecipitated with each of these proteins (Fig. 6*A*). In addition, hChlR1-HA co-immunoprecipitated endogenous p37/RFC2, one of the small subunits of the RFC and Ctf18-RFC complexes. Reciprocal immunoprecipitation experiments with the same cell lysates showed that hChlR1 was co-immunoprecipitated with Ctf18 by antisera specific for Ctf18 (Fig. 6*B*), with FLAG-Dcc1 using FLAG antibodies (Fig. 6*C*), and with Ctf8 by antisera specific for Ctf8 (data not shown). Reciprocal interactions were also detected between endogenous hChlR1 and the endogenous Ctf18 subunit (data not shown). Importantly, RFC1, the largest subunit of RFC, was not detected in hChlR1 immunoprecipitations (Fig. 6*D*), suggesting that under the conditions used, interactions between hChlR1 and the Ctf18-RFC complex may be specific. It should be noted that the interactions

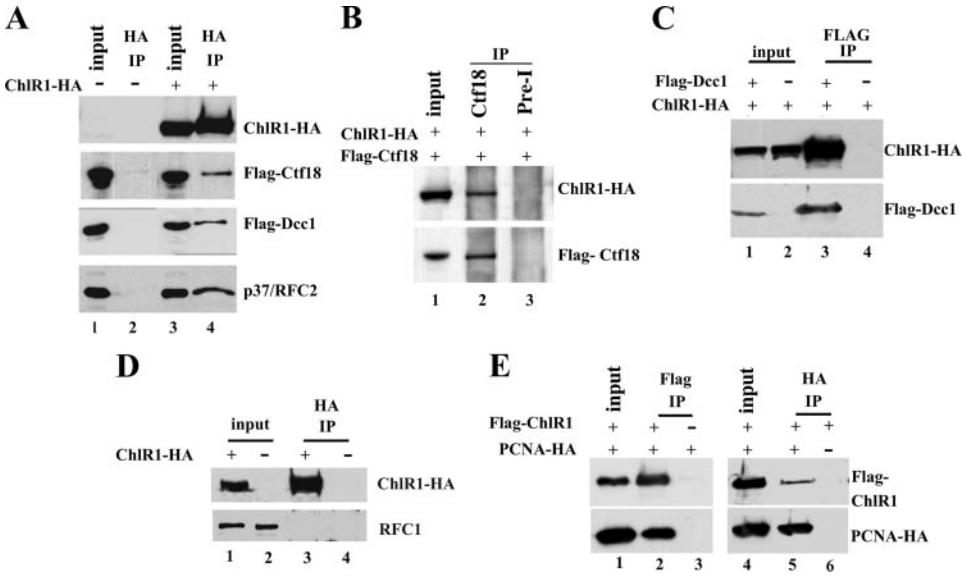

FIGURE 6. **hChlR1 interacts with the Ctf18-RFC complex and PCNA.** *A*, in the *three upper panels*, 1 mg of lysates from 293 cells transiently expressing FLAG-Ctf18 (*second panel* from *top*) or FLAG-Dcc1 (*third panel* from *top*) alone (*lane 2*) or together with constitutively expressed ChlR1-HA (lane 4) were incubated with HA antibody as indicated at the *top* of the *immunoblots*; specific interactions were detected by Western blotting, using antibodies to hChlR1 (*top panel*), Ctf18 (*second panel* from *top*), or Dcc1 (*third panel* from *top*). In the *bottom panel*, lysates from 293 cells (*lanes 2*) or 293 cells constitutively expressing ChlR1-HA (*lanes 4*) were incubated with HA antibody, and specific interactions between ChlR1-HA and endogenous p37/RFC2 subunit were detected by Western blotting using p37/RFC2 antibody. *B*, reciprocal immunoprecipitations in 293 cells expressing both ChlR1-HA and FLAG-tagged Ctf18 performed with protein A beads in combination with antibodies specific for Ctf18 (*lane 2*) or with preimmune serum (*lane 3*), as indicated at the *top* of the *immunoblot*; specific interactions were detected by Western blotting using antibodies to hChlR1 (*top*) and Ctf18 (*bottom*). *C*, immunoprecipitation using FLAG beads of lysates from 293 cells transiently expressing ChlR1-HA alone (*lane 4*) or together with FLAG-tagged Dcc1 (*lane 3*); specific interactions were detected by Western blotting using antibodies to hChlR1 (*top*) and Dcc1 (*bottom*). *D*, hChlR1 does not interact with RFC1. Lysates from 293 cells constitutively expressing ChlR1-HA (*lane 3*) were incubated with HA antibody; no specific interaction was detected by Western blotting using antibodies to hChlR1 (*top*) and the RFC1 subunit (*bottom*). *E*, hChlR1 interacts with PCNA. *Left*, 1 mg of 293 cell lysates transiently expressing FLAG-ChlR1 (*lane 2*) or 293 cell lysates (*lane 3*), supplemented with recombinant HA-PCNA (5.6 pmol) were incubated with FLAG-M2 antibody beads; *right*, 1 mg of 293 cell lysates transiently expressing FLAG-ChlR1 in the presence (*lane 5*) or absence (*lane 6*) of recombinant HA-PCNA (5.6 pmol) were incubated with HA antibody beads; specific interactions were detected by Western blotting using antibodies to hChlR1 (*top*) and PCNA (*bottom*). In all immunoprecipitations, input represents 10% of the total amount of lysate/recombinant protein used for immunoprecipitation. *IP*, immunoprecipitation.

between hChlR1 and individual subunits of the Ctf18-RFC complex are likely to include other components that make up this alternative clamp loader.

We also examined whether hChlR1 associated with PCNA. As shown in Fig. 6*E*, FLAG-tagged hChlR1 and recombinant PCNA-HA co-immunoprecipitated from 293 cell lysates. The association of hChlR1 with Ctf18-RFC and PCNA was also observed *in vitro* using recombinant proteins (data not shown). Interactions between Ctf18-RFC and PCNA have been well documented in previous studies and were shown to support PCNA loading onto DNA both *in vitro* (20–22) and *in vivo* (23, 35).

hChlR1 Interacts with Fen1 and Stimulates Its Flap Endonuclease Activity—We investigated whether hChlR1 affected the processing of lagging strand. This approach was initiated because a number of the establishment factors interact with lagging strand components (22), and genetic interactions between budding yeast Chl1 and Dna2 were detected.[4] However, no biochemical or physical interactions between hDna2 and hChlR1 were observed.[5] During these studies, we also examined whether such interactions occurred between Fen1 and hChlR1. As shown in Fig. 7, hChlR1 interacted with Fen1 and stimulated the endonuclease activity of Fen1. HA-tagged hChlR1 and FLAG-tagged Fen1, present in lysates derived from cells ectopically expressing these proteins, were co-immunoprecipitated with either HA or Fen1 antibodies (Fig. 7, *A* and *B*, respectively). The specificity of these interactions was verified by control experiments shown in Fig. 7, *A* and *B*. *In vitro* interactions between Fen1 and hChlR1 were also observed with isolated recombinant proteins (Fig. 7*C*).

We next examined whether recombinant hChlR1 affected the Fen1-catalyzed cleavage of an equilibrating flap oligonucleotide substrate (Fig. 7*D*). In the presence of low levels of Fen1 (5 fmol), increasing concentrations of hChlR1 stimulated the cleavage reaction ~3-fold. When RPA was added to reactions, the Fen1-mediated cleavage in the absence of hChlR1 was reduced (6-fold), as previously reported (36). Supplementation of such reactions with hChlR1 resulted in a marked stimulation of the cleavage reaction (~11-fold). These experiments were carried out at high molar ratios of hChlR1 to Fen1 (9–36:1). In other experiments carried out in the presence of RPA, a molar ratio of 5:1 stimulated the Fen1 cleavage reaction 2-fold. The relatively weak or poor physical interaction between Fen1 and hChlR1 observed both *in vivo* and *in vitro* (Fig. 7, *A–C*) may contribute to the high levels of hChlR1 required to increase the nuclease activity of Fen1. This effect of hChlR1, however, appeared to be independent of its helicase activity, since ATP addition was not required for the stimulation and the Walker A box mutant of hChlR1 (KRm, devoid of helicase activity) was as effective as wild-type hChlR1 (data not shown). These findings suggest that hChlR1 may contribute to the processing of lagging strands by stimulating the removal of 5′-flap structures by Fen1. hChlR1 can bind to single-stranded DNA regions 5 nt or greater (Fig. 4*B*). This property, combined with its ability to interact with Fen1, may help target Fen1 to single-stranded flap structures and explain why the helicase activity of hChlR1 appears to play no role in stimulating the endonuclease activity of Fen1. The

[4] Y. H. Kang and S.-S. Seo, unpublished results.

[5] A. Farina, J.-H. Shin, D.-H. Kim, V. P. Bermudez, Z. Kelman, Y.-S. Seo, and J. Hurwitz, unpublished results.

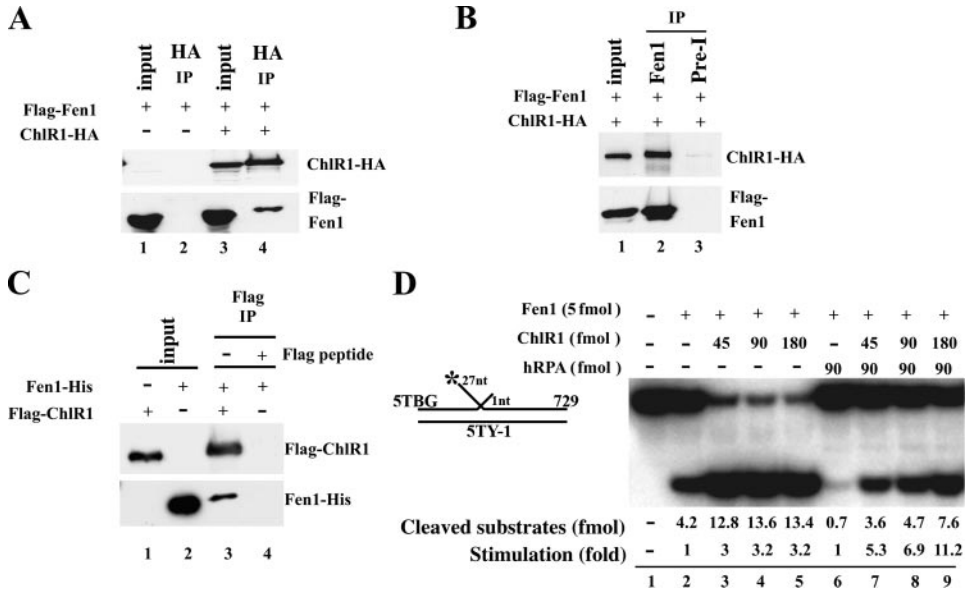

FIGURE 7. **hChlR1 interacts with Fen1 and stimulates its endonuclease activity.** *A*, 1 mg of lysates from 293 cells transiently expressing FLAG-Fen1 alone (*lane 2*) or together with constitutively expressed ChlR1-HA (*lane 4*) were incubated with HA antibody as indicated at the *top* of the *immunoblots*; specific interactions were detected by Western blotting using antibodies to hChlR1 (*top*) and Fen1 (*bottom*). *B*, reciprocal immunoprecipitations in 293 cells expressing ChlR1-HA and FLAG-tagged Fen1 performed with protein A beads in combination with Fen1 antibodies (*lane 2*) or preimmune serum (*lane 3*), as noted at the *top* of the *immunoblot*; specific interactions were detected by Western blotting using antibodies to hChlR1 (*top*), and Fen1 (*bottom*). *C*, hChlR1 directly interacts with Fen1. Recombinant His-tagged-Fen1 (5.6 pmol) and recombinant FLAG-tagged ChlR1 (5 pmol) were incubated with FLAG-M2 antibody beads (*lanes 3* and *4*); proteins were eluted in the absence (*lane 3*) or presence (*lane 4*) of 1 mg/ml FLAG peptide, and specific interactions were detected by Western blotting using antibodies specific to hChlR1 (*top*) and Fen1 (*bottom*). Input represents 10% of total amount of lysate/recombinant protein used for immunoprecipitation. *D*, hChlR1 stimulates Fen1 endonuclease activity. Fen1 (5 fmol) was incubated in the absence (*lanes 2–5*) or presence (*lanes 6–9*) of the indicated amounts of RPA with or without hChlR1 (*lanes 7–9* and *lanes 3–5*, respectively) in standard flap endonuclease reaction mixtures (described in Ref. 36) in the presence of the 729/5TBG substrate (described in Table 1), whose structure is shown on the *left*. *IP*, immunoprecipitation.

physiological relevance of the interaction of hChlR1 with Fen1 and its effect on the activity of Fen1 is presently unclear. However, these findings prompted us to examine the possible role of Fen1 in sister chromatid pairing, as described below.

Down-regulation of hChlR1 and Fen1 in HeLa Cells by siRNA Leads to Defects in Sister Chromatid Cohesion—Recently, hChlR1 was shown to be required for sister chromatid cohesion in higher eukaryotes (26). We also investigated whether hChlR1, like components of the cohesin complex, contributes to normal chromosome dynamics. Experiments were carried out in which a number of specific proteins were down-regulated by siRNA treatment (Fig. 8). We examined three proteins, hChlR1, Fen1, and the cohesin subunit Scc1. siRNAs directed specifically at the expression of these proteins in HeLa cells resulted in their marked reduction (>90% in each case; Fig. 8*C*). Microscopy of 4′,6-diamidino-2-phenylindole-stained metaphase chromosomes spread from siRNA-treated cells, 48 h following transfection, revealed chromatids either loosely paired (shown with hChlR1-depleted cells) or more widely separated (cells in which Fen1 and Scc1 were depleted), compared with the tight association noted between chromosome pairs in control spreads (Fig. 8*A*). In order to quantify these results, FISH analyses were carried out with probes specific for the centromeric region of chromosome 9 (Fig. 8*B*, *top*). The detection of a single fluorescent spot represented the presence of tightly paired chromatids in which the probe on each centromere of chromosome 9 was not resolved by fluorescent microscopy. The detection of two fluorescent spots indicated separation of the specific centromere regions in chromosome 9. The separation of chromatids was quantitated by measuring the distance between the fluorescent signals (Fig. 8*B*, *bottom*). For these measurements, 100 individual chromosome pairs were scored, and the extent of their separation was divided arbitrarily into three categories: those that showed a normal distance between chromatids (0.2–0.6 μm), those with mild defects (0.6–1.6 μm), and those with strong defects (>1.6 μm). In control cells (exposed to random siRNA), the distances between the chromosomes scored were normal (92%); the chromosomes of cells treated with siRNA directed at the cohesin subunit Scc1 showed the strongest effect, reflected by the largest separation of chromatid pairs at the centromere; cells in which Fen1p was down-regulated were affected more than cells treated with siRNA directed against hChlR1. These findings are in keeping with previous reports that depletion of Scc1 or hChlR1 leads to abnormal sister chromatid cohesion (26). The results described in the legend to Fig. 8 suggest that depletion of Fen1p, as shown by increased separation of chromatid pairs at the centromere, also leads to abnormal cohesion. In all depletion studies carried out, the level of bromodeoxyuridine incorporation into DNA was monitored as well. These measurements indicated that the levels of bulk DNA synthesized in cells depleted of hChlR1, Fen1, or Scc1 were virtually identical to that observed in control cells (data not shown).

DISCUSSION

In this report, we described the purification of hChlR1 overexpressed in human cells and characterization of some of the properties of its helicase and DNA-dependent ATPase activities. Our findings suggest that hChlR1 binds to the 5′-single-stranded region of a partial duplex DNA structure and translocates along ssDNA in a 5′–3′ direction. In order to initiate its unwinding activity, hChlR1 does not require a free 5′-end, since it can bind and unwind from a gapped ssDNA region 10 nt in length. This property may have significant physiological relevance in the processing of lagging strand structures and/or altered forklike structures formed during replication. In the presence of ATP, hChlR1 can unwind duplex DNA regions up to 100 bp; reactions supplemented with RPA or the cohesion PCNA-clamp loading complex Ctf18-RFC extended unwinding to 500 bp. All of these activities are intrinsic to hChlR1,

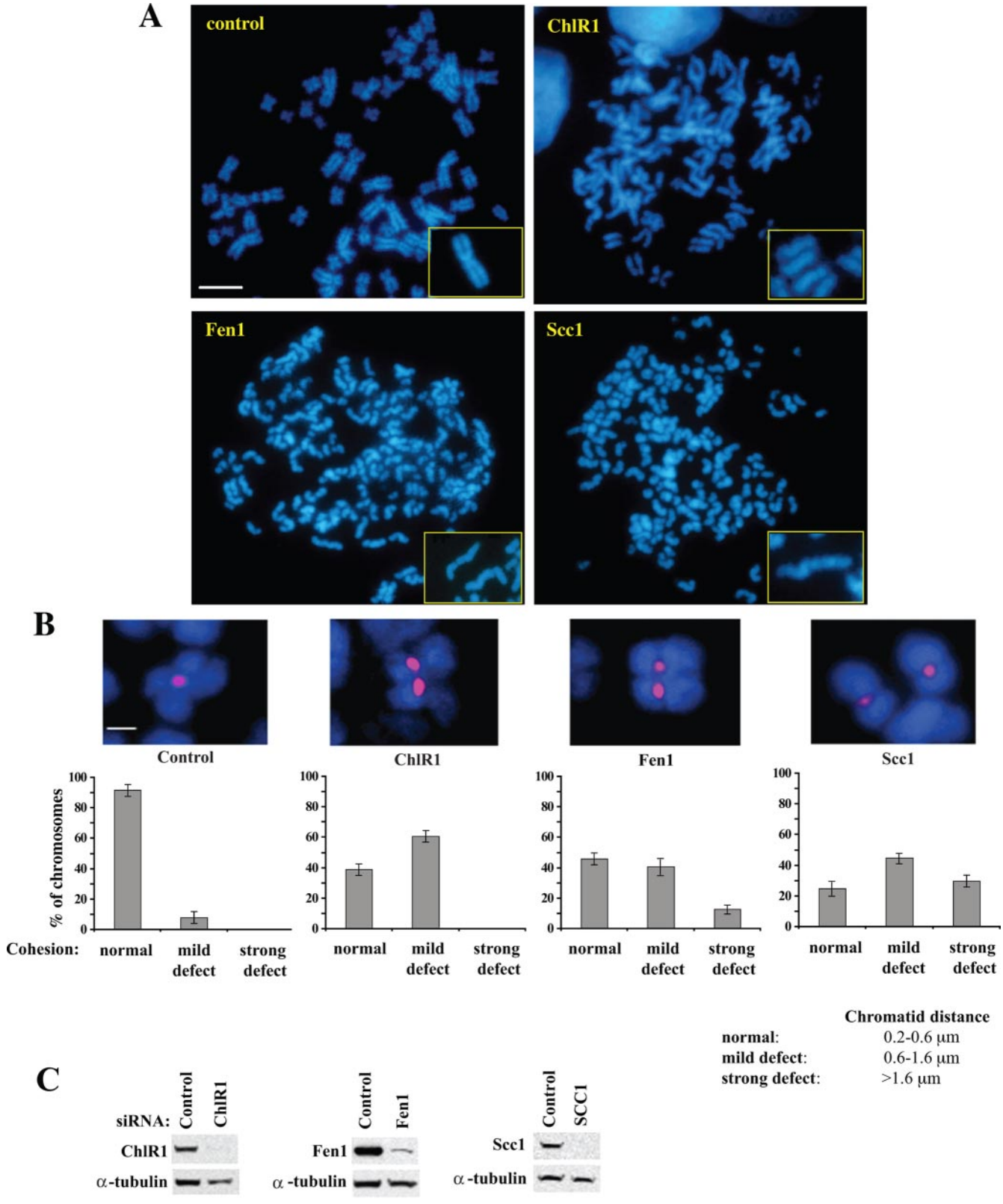

FIGURE 8. **siRNA-mediated depletion of hChlR1, Fen1, or Scc1 leads to defects in sister chromatid pairing.** *A*, HeLa cells were transfected with control (aspecific siRNA) or hChlR1-, Fen1-, or Scc1-specific siRNAs and metaphase spreads prepared 48 h following transfection. DNA was stained with 4′,6-diamidino-2-phenylindole, whereas the *inset* shown to the *right* represents a higher magnification of a sister chromatid pair; the *size reference bar* shown is 3 μm long. *B* (*top*), the centromeric region of chromosome 9 was probed using the FISH procedure (33), DNA was stained with 4′,6-diamidino-2-phenylindole, and chromosomes were visualized by microscopy; the *size reference bar* shown is 1 μm. *Bottom*, the distance between chromatid pairs of at least 100 chromosomes in each case was measured using MetaMorph software and grouped together by the distance separating the sister chromatid as shown in the *lower right side* of the figure. The results are expressed as the mean percentage of cells ± S.D. of the experiment performed in triplicate. *C*, an aliquot of cells from each siRNA experiment was harvested and subjected to Western blot analysis to determine the expression of hChlR1, Fen1, and Scc1 proteins using antibodies specific for each protein. α-Tubulin was included as loading control.

since a mutation in its Walker A motif abolished both its helicase and ATPase activities.

A wealth of data, derived primarily from studies in budding yeast, indicate that the establishment of sister chromatid cohesion occurs during S phase (6, 23). Key to this process is the role played by the four-subunit ring-shaped cohesin complex, which is loaded onto DNA prior to the onset of replication and topologically links the replicated chromosomes formed after fork passage. Stable sister chromatid cohesion requires, in addition to the cohesin complex, the action of a number of auxiliary factors, including the two examined here, Ctf18-RFC and hChlR1. Recent studies in human and mouse cells (26, 27) showed that depletion of hChlR1 by RNA interference leads to precocious separation of chromatid pairs and abnormal sister chromatid cohesion, and we have confirmed these findings. Skibbens (18) reported that in *S. cerevisiae*, Chl1 interacts genetically with Ctf18 and also showed that although Chl1 and Ctf18 are each nonessential gene products, loss of both functions is lethal. Our findings add further significance to these genetic observations, since both proteins interact physically *in vivo* and *in vitro*, and Ctf18-RFC stimulates the length of DNA unwound by hChlR1. It is likely that these effects are due to interactions between the Ctf18 subunit and hChlR1 rather than the small clamp loader subunits (RFC2 to -5), since interactions between RFC and hChlR1 were not detected, and the stimulation of the displacement of longer DNA chains by hChlR1 was much more pronounced with Ctf18-RFC than with RFC. Under the conditions used (Fig. 5), the five- and seven-subunit Ctf18-RFC complexes were equally effective in increasing the processivity of hChlR1, suggesting that the Dcc1 and Ctf8 subunits are not required for this effect. Furthermore, no differences were noted in the loading of PCNA onto DNA with either the yeast or human five- or seven-subunit Ctf18 RFC complexes (20–22), suggesting that Ctf8 and Dcc1 play no discernable role in the clamp loading reaction. Thus, although Ctf8 and Dcc1 are required for cohesion establishment in budding yeast, their contributions to cohesion remain unclear.

Although hChlR1 interacts with PCNA, the clamp alone, as well as that loaded onto DNA, did not affect the unwinding or DNA-dependent ATPase activities of the helicase (Fig. 5*B*) (data not shown). In the presence of either RFC or Ctf18-RFC, high PCNA levels inhibited the helicase activity, possibly by stabilizing the clamp loader complex at the 3′-primer end-template junction, which may block the 5′–3′ translocation of the helicase loaded onto the M13-mp18(+) strand through the duplex.

A number of the establishment factors interact genetically with a variety of lagging strand replication genes (36, 37). These findings prompted us to determine whether hChlR1 interacted with lagging strand-processing proteins. As described above, physical and biochemical interactions with Fen1 were observed. hChlR1 stimulated the Fen1-catalyzed cleavage of equilibrating flap DNA structures. We also examined whether siRNA-mediated depletion of Fen1 in HeLa cells, like that observed upon depletion of hChlR1, affected sister chromatid pairing. As shown in Fig. 8, this treatment resulted in the marked decrease of Fen1 (>90%) and an increased separation of sister chromatids. Fen1 is an essential protein in higher eukaryotes, in contrast to its conditional role in budding yeast (38). We examined bulk DNA replication in Fen1 siRNA-treated cells and noted that the level of DNA replication (scored by bromodeoxyuridine incorporation) appeared normal. Possibly, the residual level of Fen1 remaining after siRNA depletion was ample to satisfy its essential role. It is not clear whether Fen1 participates in cohesion directly or indirectly through its interaction with hChlR1. The data presented in Figs. 7 and 8 suggest that increased processing of lagging strands may be important in the establishment of cohesion. Although these findings suggest a role for hChlR1 in lagging strand replication, they do not exclude the possibility that other functions contribute to its role as a cohesion establishment factor.

Two models have been proposed for the establishment of cohesion during replication fork passage (23, 39). In one, the replication machinery slides directly through the 35-nm diameter central hole of the cohesin ring (loaded onto DNA prior to the onset of replication), ensuring that the two sister chromatids remain attached until mitosis. In the second model, it was suggested that cohesin might transiently lose its closed topological encirclement of DNA when encountered by the replication fork. In this model, the cohesion establishment factors may maintain the association of the cohesin ring with the replication fork and promote the reassociation of cohesin with the replicated products. Both models lead to sister chromatids enclosed within the cohesin ring complex, following passage of the replication fork. There are substantial data supporting the topological linkage of sister chromatids with cohesin and the notion that no newly loaded cohesin is required to support cohesion after DNA replication has been initiated (23, 39). Further support that cohesin is loaded around chromatin is derived from the observations that the cohesin complex can slide along chromatin, before and after DNA replication (23). In budding yeast, active transcription appears to relocalize cohesin to intergenic regions, suggesting that the transcription machinery is too large to pass through the cohesin ring. In contrast, there are no data suggesting that replication alters the positioning of cohesin (23). Although calculations of the size of a replication fork suggest it may be small enough to pass through a cohesin ring (22, 23), it is likely that a lagging strand region with an extruded loop, as proposed in the trombone model, is too large to pass through the cohesin ring. The lengths of such loops, based on direct electron microscopy measurements of such structures formed during T4 or T7 DNA replication, are >100 nm (40, 41), much too large to pass through a 35-nm diameter of a cohesin ring. A model addressing this problem has been proposed by Bylund and Burgers (22). Key to this model is the relaxation of the lagging strand loop and generation of linear lagging strand structures that can pass through the cohesin ring. They proposed that PCNA clamps loaded on lagging strands are important structures that organize the replisome and suggested that Ctf18-RFC catalyzes the unloading of PCNA from lagging strand trombone structures, which leads to their collapse and passage of the fork through the cohesin ring. This proposal is weakened by the finding that in budding yeast, deletion of Ctf18 markedly decreased the levels of PCNA present in the vicinity of replication forks (23). We consider another model that also involves replisome passage through the cohesin ring. We sug-

gest that upon encountering cohesin, the trombone loop structure is trapped and remodeled by the concerted action of establishment factors and replication proteins located at the fork. Completion of lagging strand synthesis between two Okazaki fragments would remove the loop structure and permit passage of the fork complexed to its replicated sister chromatid through the cohesin ring. We suggest that PCNA accumulated on the lagging strand contributes to this targeted completion of the lagging strand loop. In keeping with this notion, a number of the establishment factors have been shown to interact with PCNA (Ctf7p (42), hChlR1, and Ctf18-RFC) and function in lagging strand synthesis (interaction of DNA polymerase α with Ctf4 (43, 44); Fen1 through its interaction with hChlR1). It is evident that a more precise characterization of the biochemical properties of the establishment factors will help define how they participate in cohesion. Their specific role in cohesion, however, awaits the development of cell-free systems capable of loading cohesin onto DNA as well as supporting replication.

Acknowledgment—We are grateful to Inger Tappin for technical support.

REFERENCES

1. Guacci, V., Koshland, D., and Strunnikov, A. (1997) *Cell* **91,** 47–57
2. Michaelis, C., Ciosk, R., and Nasmyth, K. (1997) *Cell* **91,** 35–45
3. Losada, A., Hirano, M., and Hirano, T. (1998) *Genes Dev.* **12,** 1986–1997
4. Haering, C. H., Lowe, J., Hochwagen, A., and Nasmyth, K. (2002) *Mol. Cell* **9,** 773–788
5. Chestukhin, A., Pfeffer, C., Milligan, S., DeCaprio, J. A., and Pellman, D. (2003) *Proc. Natl. Acad. Sci. U. S. A.* **100,** 4574–4579
6. Hanna, J. S., Kroll, E. S., Lundblad, V., and Spencer, F. A. (2001) *Mol. Cell. Biol.* **21,** 3144–3158
7. Mayer, M. L., Gygi, S. P., Aebersold, R., and Hieter, P. (2001) *Mol. Cell* **7,** 959–970
8. Skibbens, R. V., Corson, L. B., Koshland, D., and Hieter, P. (1999) *Genes Dev.* **13,** 307–319
9. Tanaka, K., Yonekawa, T., Kawasaki, Y., Kai, M., Furuya, K., Iwasaki, M., Murakami, H., Yanagida, M., and Okayama, H. (2000) *Mol. Cell. Biol.* **20,** 3459–3469
10. Toth, A., Ciosk, R., Uhlmann, F., Galova, M., Schleiffer, A., and Nasmyth, K. (1999) *Genes Dev.* **13,** 320–333
11. Williams, D. R., and McIntosh, J. R. (2002) *Eukaryot. Cell* **1,** 758–773
12. Kohler, A., Schmidt-Zachmann, M. S., and Franke, W. W. (1997) *J. Cell Sci.* **110,** 1051–1062
13. Haber, J. E. (1974) *Genetics* **78,** 843–858
14. Liras, P., McCusker, J., Mascioli, S., and Haber, J. E. (1978) *Genetics* **88,** 651–671
15. Gerring, S. L., Spencer, F., and Hieter, P. (1990) *EMBO J.* **9,** 4347–4358
16. Holloway, S. L. (2000) *Nucleic Acids Res.* **28,** 3056–3064
17. Amann, J., Kidd, V. J., and Lahti, J. M. (1997) *J. Biol. Chem.* **272,** 3823–3832
18. Skibbens, R. V. (2004) *Genetics* **166,** 33–42
19. Waga, S., and Stillman, B. (1998) *Annu. Rev. Biochem.* **67,** 721–751
20. Bermudez, V. P., Maniwa, Y., Tappin, I., Ozato, K., Yokomori, K., and Hurwitz, J. (2003) *Proc. Natl. Acad. Sci. U. S. A.* **100,** 10237–10242
21. Shiomi, Y., Shinozaki, A., Sugimoto, K., Usukura, J., Obuse, C., and Tsurimoto, T. (2004) *Genes Cells* **9,** 279–290
22. Bylund, G. O., and Burgers, P. M. (2005) *Mol. Cell. Biol.* **25,** 5445–5455
23. Lengronne, A., McIntyre, J., Katou, Y., Kanoh, Y., Hopfner, K. P., Shirahige, K., and Uhlmann, F. (2006) *Mol. Cell* **23,** 787–799
24. Mayer, M. L., Pot, I., Chang, M., Xu, H., Aneliunas, V., Kwok, T., Newitt, R., Aebersold, R., Boone, C., Brown, G. W., and Hieter, P. (2004) *Mol. Biol. Cell* **15,** 1736–1745
25. Petronczki, M., Chwalla, B., Siomos, M. F., Yokobayashi, S., Helmhart, W., Deutschbauer, A. M., Davis, R. W., Watanabe, Y., and Nasmyth, K. (2004) *J. Cell Sci.* **117,** 3547–3559
26. Parish, J. L., Rosa, J., Wang, X., Lahti, J. M., Doxsey, S. J., and Androphy, E. J. (2006) *J. Cell Sci.* **119,** 4857–4865
27. Inoue, A., Li, T., Roby, S. K., Valentine, M. B., Inoue, M., Boyd, K., Kidd, V. J., and Lahti, J. M. (2007) *Cell Cycle* **6,** 1646–1654
28. Ishiai, M., Sanchez, J. P., Amin, A. A., Murakami, Y., and Hurwitz, J. (1996) *J. Biol. Chem.* **271,** 20868–20878
29. Uhlmann, F., Cai, J., Flores-Rozas, H., Dean, F. B., Finkelstein, J., O'Donnell, M., and Hurwitz, J. (1996) *Proc. Natl. Acad. Sci. U. S. A.* **93,** 6521–6526
30. Rocchi, M., Archidiacono, N., Ward, D. C., and Baldini, A. (1991) *Genomics* **9,** 517–523
31. Shin, J. H., Jiang, Y., Grabowski, B., Hurwitz, J., and Kelman, Z. (2003) *J. Biol. Chem.* **278,** 49053–49062
32. Lee, J. K., and Hurwitz, J. (2001) *Proc. Natl. Acad. Sci. U. S. A.* **98,** 54–59
33. Leversha, M. A. (2001) *Methods Mol. Biol.* **175,** 109–127
34. Hirota, Y., and Lahti, J. M. (2000) *Nucleic Acids Res.* **28,** 917–924
35. Kim, J., Robertson, K., Mylonas, K. J., Gray, F. C., Charapitsa, I., and MacNeill, S. A. (2005) *Nucleic Acids Res.* **33,** 4078–4089
36. Kim, J. H., Kim, H. D., Ryu, G. H., Kim, D. H., Hurwitz, J., and Seo, Y. S. (2006) *Nucleic Acids Res.* **34,** 1854–1864
37. Tsutsui, Y., Morishita, T., Natsume, T., Yamashita, K., Iwasaki, H., Yamao, F., and Shinagawa, H. (2005) *Curr. Genet.* **48,** 34–43
38. Zheng, L., Dai, H., Qiu, J., Huang, Q., and Shen, B. (2007) *Mol. Cell. Biol.* **27,** 3176–3186
39. Nasmyth, K., and Haering, C. H. (2005) *Annu. Rev. Biochem.* **74,** 595–648
40. Chastain, P. D., II, Makhov, A. M., Nossal, N. G., and Griffith, J. (2003) *J. Biol. Chem.* **278,** 21276–21285
41. Moldovan, G. L., Pfander, B., and Jentsch, S. (2006) *Mol. Cell* **23,** 723–732
42. Park, K., Debyser, Z., Tabor, S., Richardson, C. C., and Griffith, J. D. (1998) *J. Biol. Chem.* **273,** 5260–5270
43. Zhu, W., Ukomadu, C., Jha, S., Senga, T., Dhar, S. K., Wohlschlegel, J. A., Nutt, L. K., Kornbluth, S., and Dutta, A. (2007) *Genes Dev.* **21,** 2288–2299
44. Wittmeyer, J., and Formosa, T. (1997) *Mol. Cell. Biol.* **17,** 4178–4190